Acta Pharmacologica Sinica

www.nature.com/aps

ARTICLE

Pyrroloquinoline quinone promotes mitochondrial biogenesis in rotenone-induced Parkinson's disease model via AMPK activation

Qiong Cheng[1], Juan Chen[1], Hui Guo[1], Jin-li Lu[1], Jing Zhou[1], Xin-yu Guo[2], Yue Shi[2], Yu Zhang[2], Shu Yu[1], Qi Zhang[1] and Fei Ding[1,3]

Mitochondrial dysfunction is considered to be one of the important pathogenesis in Parkinson's disease (PD). We previously showed that pyrroloquinoline quinone (PQQ) could protect SH-SY5Y cells and dopaminergic neurons from cytotoxicity and prevent mitochondrial dysfunction in rotenone-induced PD models. In the present study we investigated the mechanisms underlying the protective effects of PQQ in a mouse PD model, which was established by intraperitoneal injection of rotenone (3 mg·kg^{-1}·d^{-1}, ip) for 3 weeks. Meanwhile the mice were treated with PQQ (0.8, 4, 20 mg·kg^{-1}·d^{-1}, ip) right after rotenone injection for 3 weeks. We showed that PQQ treatment dose-dependently alleviated the locomotor deficits and nigral dopaminergic neuron loss in PD mice. Furthermore, PQQ treatment significantly diminished the reduction of mitochondria number and their pathological change in the midbrain. PQQ dose-dependently blocked rotenone-caused reduction in the expression of PGC-1α and TFAM, two key activators of mitochondrial gene transcription, in the midbrain. In rotenone-injured human neuroblastoma SH-SY5Y cells, PTMScan Direct analysis revealed that treatment with PQQ (100 μM) differentially regulated protein phosphorylation; the differentially expressed phosphorylated proteins included the signaling pathways related with adenosine 5′-monophosphate (AMP)-activated protein kinase (AMPK) pathway. We conducted Western blot analysis and confirmed that AMPK was activated by PQQ both in PD mice and in rotenone-injured SH-SY5Y cells. Pretreatment with AMPK inhibitor dorsomorphin (4 μM) significantly attenuated the protective effect and mitochondrial biogenesis by PQQ treatment in rotenone-injured SH-SY5Y cells. Taken together, PQQ promotes mitochondrial biogenesis in rotenone-injured mice and SH-SY5Y cells via activation of AMPK signaling pathway.

Keywords: Parkinson's disease; rotenone pyrroloquinoline quinone; mitochondrial biogenesis; AMPK; PTMScan Direct analysis

Acta Pharmacologica Sinica (2021) 42:665–678; https://doi.org/10.1038/s41401-020-0487-2

INTRODUCTION

Parkinson's disease (PD), the second most common neurodegenerative disease, is characterized by the substantial loss of dopaminergic neurons in the substantia nigra pars compacta (SNpc), accompanied by motor impairments, such as tremor, rigidity and bradykinesia, and nonmotor symptoms [1]. Although mitochondrial dysfunction is considered to be one of the molecular pathologies in PD, the mechanisms have still not been clearly elucidated.

Mitochondrial biogenesis plays an important role in neurodegeneration and is regulated by several cell signaling pathways, including the AMP-activated protein kinase (AMPK)/peroxisome proliferator–activated receptor gamma coactivator-1α (PGC-1α) and sirtuin 1 (SIRT1)/PGC-1α pathways [2, 3]. The suppressive activity of PGC-1α, a master mitochondrial biogenesis regulator, is considered the main cause of familial PD induced by PTEN induced putative kinase 1 (PINK1) and parkin mutations [3]. Therefore, the development of new drugs targeting mitochondrial biogenesis seems to have potential applications for PD treatment [4].

Rotenone is widely used to establish PD models in rodents [5, 6], as it reproduces the pathological hallmarks of PD as well as some parkinsonian motor deficits [7, 8]. Systemic administration of rotenone induced chronic progressive degeneration of the nigrostriatal pathway and α-synuclein pathology in rats, similar to observations in PD patients [5, 9]. Both human PD and chronic rotenone exposure lead to dopaminergic axon loss followed by cell death [10]. Our previous study indicated that pyrroloquinoline quinone (PQQ), a redox cofactor targeting mitochondrial respiratory chain complexes I and III, could antagonize rotenone-induced cell injury both in vitro and in vivo [11–13], suggesting that PQQ might be a candidate for PD treatment through its regulation of mitochondrial functions.

Posttranslational modifications (PTMs) are increasingly recognized as crucial mechanisms in PD pathogenesis, as many important proteins involved in PD, such as α-synuclein and leucine-rich repeat kinase 2 (LRRK2), are modulated by PTMs, which affect cellular functions by regulating protein stability, localization and function [14, 15]. Recently, some drugs and

[1]Key Laboratory of Neuroregeneration of Jiangsu and Ministry of Education, Co-innovation Center of Neuroregeneration, Nantong University, Nantong 226001, China; [2]School of Medicine, Nantong University, Nantong 226001, China and [3]Jiangsu Clinical Medicine Center of Tissue Engineering and Nerve Injury Repair, Nantong 226001, China
Correspondence: Qi Zhang (zhangqi@ntu.edu.cn) or Fei Ding (dingfei@ntu.edu.cn)
These authors contributed equally: Qiong Cheng, Juan Chen

Received: 26 February 2020 Accepted: 19 July 2020
Published online: 28 August 2020

molecules were found to exert protective effects in PD models by regulating protein phosphorylation, acetylation, methylation or ubiquitination [1, 8, 16, 17]. Our previous studies also suggested that PQQ could phosphorylate extracellular regulated protein kinases (ERKs) and members of the phosphatidylinositol-3-kinase (PI3K)/protein serine-threonine kinase (AKT) signaling pathways to protect SH-SY5Y cells and dopaminergic neurons from rotenone injury [11, 12]. Further comprehensive investigation might be helpful to gain insight into the neuroprotective effect and mechanism of PQQ in PD models.

In the present study, a PD mouse model induced by intraperitoneal rotenone injections was used to observe the neuroprotective effect of PQQ. Moreover, an immunoaffinity-based LC-MS/MS method, PTMScan Direct analysis, was applied to identify signaling pathways that play specific roles in the effect of PQQ against rotenone injury. PTMScan Direct, an antibody-based proteomic method for the identification and quantification of hundreds of phosphorylated peptides and proteins in many different cell signaling pathways, has been employed to study mechanisms involved in neurodegenerative diseases [18, 19]. We aimed to investigate the neuroprotective effect of PQQ in a rotenone-induced PD model and to detect the changes in the protein phosphorylation profile of rotenone-injured SH-SY5Y cells induced by PQQ treatment. Our findings in a rotenone-induced PD model will provide a new understanding of the molecular mechanism involved in the neuroprotective effect of PQQ, indicating that PQQ might be a potential therapeutic target for PD treatment.

MATERIALS AND METHODS

Chemicals and antibodies

PQQ, rotenone, trypsin, monoclonal mouse anti-β-Actin antibody, and Epon 812 were purchased from Sigma-Aldrich (St. Louis, MO, USA). Polyclonal rabbit anti-p-AMPKα antibody, polyclonal rabbit anti-AMPKα antibody, the PTMScan® Multi-Pathway Enrichment Kit, HRP-conjugated goat anti-mouse IgG and HRP-conjugated donkey anti-rabbit IgG were obtained from Cell Signaling Technology (Danvers, MA, USA). Polyclonal rabbit anti-TH antibody, polyclonal rabbit anti-PGC-1α antibody, polyclonal rabbit anti-TFAM antibody and donkey anti-rabbit IgG-FITC were purchased from Abcam (Cambridge, MA, USA). Dulbecco's modified Eagle's medium (DMEM) and fetal bovine serum (FBS) were purchased from Gibco (Grand Island, NY, USA). Tissue lysis buffer, protease inhibitor cocktail, a BCA-based protein quantification kit and BeyoECL Plus were obtained from Beyotime (Shanghai, China). TRIzol reagent and MitoTracker® Green FM were purchased from Life Technologies (Carlsbad, CA, USA). Fast EvaGreen qPCR Master Mix was purchased from Biotium (Hayward, CA, USA). The Omniscript reverse transcription (RT) kit was provided by Qiagen (Valencia, CA, USA). Dorsomorphin (compound C) 2HCl was purchased from Selleck (Houston, TX, USA).

Animals

Adult ICR mice (25–30 g, male) were obtained from the Experimental Animal Center of Nantong University (China). The animal study was reviewed and approved by the Institutional Animal Care Committee of Nantong University (Nantong, China). The mice were randomly divided into five groups before drug administration and adapted to the environment for 3 days. A total of 18 mice were included in each group in the experiment. Rotenone (3 $mg{\cdot}kg^{-1}{\cdot}d^{-1}$ dissolved in normal saline with 2% DMSO) was intraperitoneally administered once daily for 3 weeks to establish a PD mouse model. PQQ at different dosages (0.8, 4, and 20 $mg{\cdot}kg^{-1}{\cdot}d^{-1}$) was intraperitoneally administered immediately after rotenone injection every day. The animals in the control group were injected with normal saline containing 2% DMSO. The body weight of each mouse was recorded every week.

For the detection of AMPK activity in PD mice, a time-course study was performed. Rotenone (3 $mg{\cdot}kg^{-1}{\cdot}d^{-1}$) was intraperitoneally administered once daily for 3 weeks. PQQ at a high dosage (20 $mg{\cdot}kg^{-1}{\cdot}d^{-1}$) was intraperitoneally administered immediately after rotenone injection. The control group was injected with normal saline containing 2% DMSO. Ten mice were used for each group. The midbrains were harvested at the end of weeks 1, 2, and 3 for protein analysis.

Behavioral tests

At the end of treatment, all mice were subjected to behavioral training for 3 consecutive days before the tests were performed. The rotarod test was used to evaluate motor coordination in PD mice using an accelerating rotarod apparatus (RWD, Shenzhen, China) as described previously [20]. The mice were trained in acceleration mode (4–40 rpm) over 5 min, and the latency before each mouse fell off the rod in the test was recorded. The pole test was applied with minimal modifications as described previously to assess bradykinesia [20]. Briefly, mice were placed with their head upward at the top of a rough wooden pole (16 mm in diameter and 60 mm in height), and the total time that each mouse took to orient downward and descend to the floor was recorded. The traction test was conducted as described previously [21]. Briefly, mice were suspended by the forepaws on a horizontal wire approximately 70 cm away from the ground. Each mouse was scored as follows: 3 points, the mouse grasped the wire with two hind limbs; 2 points, the mouse grasped the wire with one hind limb; 1 point, the mouse did not grasp the wire with either of the hind limbs. The open field test was performed, and the activity of each mouse was monitored for 30 min. The distance moved by each mouse was automatically calculated by a video tracking system. Eighteen animals in each group were used for the behavioral tests.

TH immunofluorescent staining

After the behavioral tests, the midbrains were dissected, sectioned, and incubated with anti-TH antibody (1:200) overnight at 4 °C and donkey anti-rabbit IgG-FITC (1:200) for 2 h at room temperature. The average immunostaining fluorescence intensity was measured with ImageJ software (version 1.51, NIH, Bethesda, MD, USA). Four animals in each group were used for TH staining.

Transmission electron microscopy (TEM)

The midbrains were dissected, fixed with precooled 2.5% glutaraldehyde, post fixed with a 1% osmium tetroxide solution, dehydrated stepwise with increasing concentrations of ethanol, and embedded in Epon 812 epoxy resin. Ultrathin sections were stained with lead citrate and uranyl acetate and then examined under a transmission electron microscope (JEOL Ltd., Tokyo, Japan). We classified the mitochondria into "type 1" and "type 2" based on organelle structure; "type 1" mitochondria were very packed and very electron-dense, and "type 2" mitochondria were less electron-dense and showed a reduced number of mitochondrial cristae and enlarged intracristal spaces. The "type 1" and "type 2" mitochondria were quantified. Four animals in each group were used for TEM observation. Cultured SH-SY5Y cells under different treatments were also subjected to TEM observation as described above.

Quantitative real-time reverse transcription PCR (qRT-PCR)

Total RNA was extracted from the midbrain and cortex tissues with TRIzol, and the RNA was reverse transcribed into cDNA with an Omniscript RT kit according to the manufacturer's instructions. The reaction mixture consisted of 5 μL of 2×Fast EvaGreen Master Mix, 0.5 μL of forward primer, 0.5 μL of reverse primer (Table 1), and 1 μL of cDNA. PCR amplification was performed on the StepOne real-time PCR system (Applied Biosystems, Foster City, CA, USA). The relative mRNA expression level was calculated

Table 1. Oligonucleotide sequences used in qRT-PCR analysis.

Gene	Primer sequence (5′–3′)
PGC-1α	Forward: gccttcttgctcttcctt Reverse: atcctttggggtctttga
TFAM	Forward: ttgggcacaagaagctggttaa Reverse: gcattcagtgggcagaagtcc
18 S rRNA	Forward: tagagggacaagtggcgttc Reverse: cgctgagccagtcagtgt

by the comparative $2^{-\Delta\Delta Ct}$ method and normalized against 18S rRNA.

Western blotting
The mouse midbrain and cortex and cultured SH-SY5Y cells were individually collected in RIPA lysis buffer (20 mM Tris-HCl [pH 7.5], 150 mM NaCl, 1 mM Na_2EDTA, 1 mM EGTA, 1% NP-40, 1% sodium deoxycholate, 2.5 mM sodium pyrophosphate, 1 mM β-glycerophosphate, 1 mM Na_3VO_4, 1 μg/mL leupeptin), and the protein concentration was quantified by BCA analysis, followed by electrophoretic separation by SDS-PAGE. After transfer to a PVDF membrane (Millipore, Bedford, MA), the membrane was blocked with 5% nonfat dry milk in Tris-buffered saline (TBS, pH 7.4) and incubated with anti-PGC-1α (1:500), anti-TFAM (1:500), anti-p-AMPKα (1:500), anti-AMPKα (1:500), or anti-β-Actin (1:4000) antibody at 4 °C overnight. After washing with TBS/T (TBS with 0.1% Tween 20), HRP-conjugated affinity-purified donkey anti-rabbit IgG (1:5000) or goat anti-mouse IgG (1:5000) was applied and incubated at room temperature for 1 h. The membrane was incubated with ECL substrate and scanned with an imaging system (Tanon, Shanghai, China). The data were analyzed with PDQuest 7.2.0 software (Bio-Rad, Hercules, CA, USA). β-Actin was used as an internal control to normalize protein loading.

Cell lysate preparation and PTMScan multipathway analysis
SH-SY5Y human neuroblastoma cells were cultured in DMEM supplemented with 10% FBS at 37 °C in a humidified atmosphere of 95% air and 5% CO_2. The day before treatment, cells were plated in a 10-cm culture dish at a density of 1×10^6 cells/mL. The cells were divided into four groups: the control group (no rotenone or PQQ), PQQ group (100 μM PQQ), Rotenone group (100 μM rotenone), and PQQ + Rotenone group (100 μM PQQ + 100 μM rotenone). Thirty minutes after treatment, the cells were washed once with cold PBS and scraped in urea lysis buffer (9 M sequanal-grade urea, 20 mM HEPES [pH 8.0], 1 mM β-glycerophosphate, 1 mM sodium vanadate, 2.5 mM sodium pyrophosphate). The cells were sonicated in lysis buffer and centrifuged for 15 min at 4 °C and 20,000 × *g*. Supernatants were collected and reduced with 4.5 mM DTT for 30 min at 55 °C. Reduced lysates were alkylated with iodoacetamide (0.019 g/mL of H_2O) for 15 min in the dark. The samples were diluted 1:4 with 20 mM HEPES [pH 8.0] and digested with 10 g/mL trypsin-tosylphenylalanyl chloromethyl ketone in 1 mM HCl overnight. Digested peptide lysates were acidified with 1% TFA, and the peptides were desalted over 360-mg SEP PAK Classic C18 columns (Waters, Milford, MA, USA). Peptides were eluted with 40% acetonitrile in 0.1% TFA, dried under a vacuum, and stored at −80 °C. PTMScan Direct was adapted from the PhosphoScan method developed at Cell Signaling Technology [18]. Differentially expressed phosphoproteins were identified and analyzed.

Cell viability measurements
SH-SY5Y cells were plated in a 96-well plate and treated with rotenone or rotenone and different concentrations of PQQ. The AMPK inhibitor dorsomorphin (4 μM) was applied to the cells 30 min before rotenone and PQQ treatment. Cell viability was assessed by the CCK-8 method after 24 h. The absorbance (optical density, *OD*) at 450 nm was measured by spectrophotometry with an ELx800 microplate reader (Bio-Tek Inc., Winooski, VT, USA).

MitoTracker® green staining
SH-SY5Y cells were plated in a 24-well plate and treated with rotenone or rotenone and different concentrations of PQQ. Dorsomorphin (4 μM) was applied to the cells 30 min before rotenone and PQQ treatment. Twenty-four hours after treatment, the cells were incubated with 100 nM MitoTracker® Green FM at 37 °C for 30 min, after which the cells were fixed in 3% glutaraldehyde for 30 min. Images were taken with a Leica confocal microscope, and the average fluorescence intensity was measured with ImageJ software (version 1.51, NIH, Bethesda, MD, USA).

Statistical analysis
Statistical analysis was performed by GraphPad Prism 5 software (GraphPad Software Inc., San Diego, CA, USA), and data are presented as the means ± SEMs. Differences between groups were analyzed by one-way or two-way analysis of variance (ANOVA) and subsequent Tukey's multiple comparisons test. Statistical significance was set as $P < 0.05$.

RESULTS

Effect of PQQ on locomotor activity in PD mice
PQQ at different concentrations was intraperitoneally injected for 21 consecutive days, and the effect of PQQ was observed in a rotenone-induced PD mouse model. Body weight increased steadily over the experiment with time, and no significant differences in body weight were observed between the groups (Fig. 1a). Motor functions were assessed by the rotarod test, pole test, traction test and open field at the end of injection. In the rotarod test, a significantly shorter latency to fall was observed in the rotenone (Rot) group (3 $mg{\cdot}kg^{-1}{\cdot}d^{-1}$) (38.56 ± 4.19 s) than in the control group (64.78 ± 3.76 s) (Fig. 1b). Treatment with 4 $mg{\cdot}kg^{-1}{\cdot}d^{-1}$ (62.89 ± 4.79 s) and 20 $mg{\cdot}kg^{-1}{\cdot}d^{-1}$ (57.56 ± 7.52 s) PQQ significantly prevented this decrease in latency (Fig. 1b). In the pole test, PQQ at a high dosage inhibited the increase in time spent descending from the pole, as shown by the following results (Fig. 1c): control, 12.44 ± 1.22 s; Rot, 21.44 ± 2.54 s; Rot + 0.8 $mg{\cdot}kg^{-1}{\cdot}d^{-1}$ PQQ, 16.28 ± 1.12 s; Rot + 4 $mg{\cdot}kg^{-1}{\cdot}d^{-1}$ PQQ, 15.83 ± 1.03 s; Rot + 20 $mg{\cdot}kg^{-1}{\cdot}d^{-1}$ PQQ, 14.06 ± 1.25 s. The rotenone-induced decrease of traction test score could also be rescued by 4 and 20 $mg{\cdot}kg^{-1}{\cdot}d^{-1}$ PQQ treatment, as shown by the following results (Fig. 1d): control, 2.50 ± 0.15; Rot, 1.06 ± 0.17; Rot + 0.8 $mg{\cdot}kg^{-1}{\cdot}d^{-1}$ PQQ, 1.67 ± 0.20; Rot + 4 $mg{\cdot}kg^{-1}{\cdot}d^{-1}$ PQQ, 1.83 ± 0.19; Rot + 20 $mg{\cdot}kg^{-1}{\cdot}d^{-1}$ PQQ, 1.83 ± 0.17. However, no significant differences in distance between groups were detected in the open field test (Fig. 1e): control, 8.56 ± 0.39 m; Rot, 8.30 ± 0.48 m; Rot + 0.8 $mg{\cdot}kg^{-1}{\cdot}d^{-1}$ PQQ, 8.48 ± 0.37 m; Rot + 4 $mg{\cdot}kg^{-1}{\cdot}d^{-1}$ PQQ, 7.66 ± 0.44 m; Rot + 20 $mg{\cdot}kg^{-1}{\cdot}d^{-1}$ PQQ, 8.21 ± 0.38 m. Together, the above data indicated that PQQ could improve locomotor activity in rotenone-induced PD mice.

Effect of PQQ on the loss of TH-positive nigral neurons in PD mice
To observe the effect of PQQ on neuronal loss in the SNpc, TH staining was performed, and the images are shown in Fig. 2a. The average fluorescent intensity of TH staining in the SNpc was lower in the rotenone group than in the control group, but both 4 and 20 $mg{\cdot}kg^{-1}{\cdot}d^{-1}$ PQQ treatment significantly increased the number of TH-positive cells, as shown by the following data (Fig. 2b): control, 224.70 ± 7.77; Rot, 125.00 ± 10.92; Rot + 0.8 $mg{\cdot}kg^{-1}{\cdot}d^{-1}$ PQQ, 133.30 ± 8.47; Rot + 4 $mg{\cdot}kg^{-1}{\cdot}d^{-1}$ PQQ, 176.20 ± 13.38; Rot + 20 $mg{\cdot}kg^{-1}{\cdot}d^{-1}$ PQQ, 203.10 ± 11.35. These data suggested that PQQ could inhibit neuronal loss in the SNpc of PD mice, which might be responsible for the rescue of motor functions observed in behavioral tests.

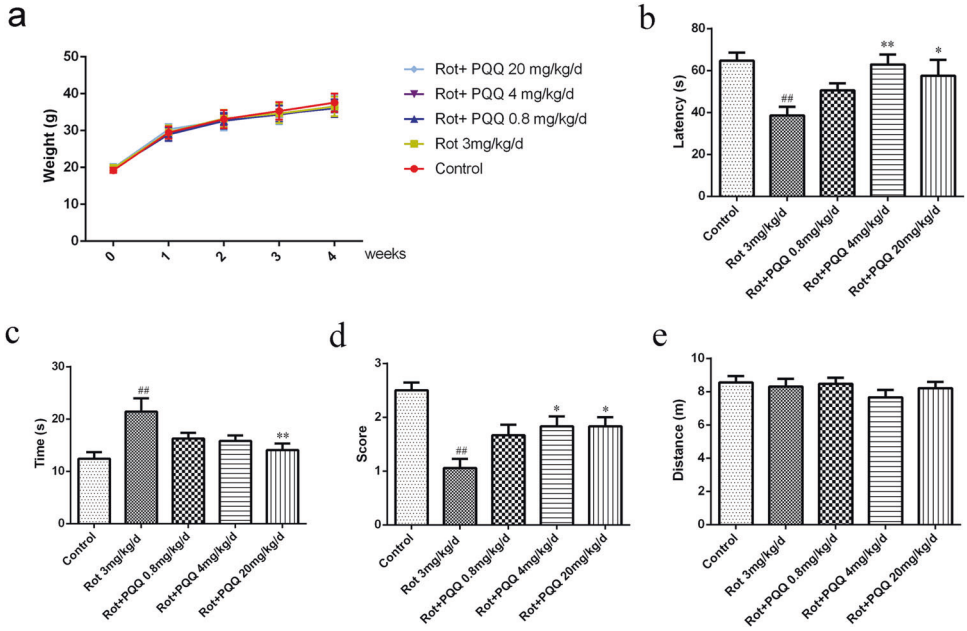

Fig. 1 PQQ alleviated rotenone-induced locomotor deficits in mice. Rotenone (3 mg·kg^{-1}·d^{-1} dissolved in normal saline with 2% DMSO) was intraperitoneally injected into ICR mice for 21 consecutive days, and PQQ at different doses was simultaneously injected. The mice were divided into the control group (Control), rotenone injury group (Rot), low-dosage PQQ group (Rot + 0.8 mg·kg^{-1}·d^{-1} PQQ), medium-dosage PQQ group (Rot + 4 mg·kg^{-1}·d^{-1} PQQ), and high-dosage PQQ group (Rot + 20 mg·kg^{-1}·d^{-1} PQQ). Normal saline with 2% DMSO was used in the control group. **a** Body weight change after rotenone and PQQ treatment. **b** Average time of latency for the mice to fall in the rotarod test. **c** Total time for each mouse to orient downward and descend to the floor in the pole test. **d** Score in the traction test. **e** Distance measured in the open field test. Data are represented as the mean ± SEM ($n = 18$ for each group). *$P < 0.05$ and **$P < 0.01$ vs the Rot group. $^{\#\#}P < 0.01$ vs the control group.

Effect of PQQ on mitochondrial biogenesis in PD mice

To evaluate the impact of PQQ on mitochondrial biogenesis in rotenone-induced PD mice, the ultrastructure of mitochondria in the midbrain neurons was observed by electron microscopy. In the control group, most mitochondria showed a normal structure and, because they were packed and electron-dense, were classified as "type 1" mitochondria. After rotenone-induced injury, the total number of mitochondria decreased, and some mitochondria displayed a pathological morphology, such as incomplete membranes, vacuoles in the matrix, enlarged intercristal spaces and increased mitochondrial size with swelling, and were thus classified as "type 2" mitochondria (Fig. 3a). Although treatment with only 20 mg·kg^{-1}·d^{-1} PQQ decreased the number of "type 2" mitochondria (6.23 ± 0.33 per 100 μm^2) compared with that in the rotenone group (9.77 ± 0.70 per 100 μm^2), treatment with PQQ at all doses (Rot + 0.8 mg·kg^{-1}·d^{-1} PQQ, 27.86 ± 1.02; Rot + 4 mg·kg^{-1}·d^{-1} PQQ, 32.68 ± 1.80; Rot + 20 mg·kg^{-1}·d^{-1} PQQ, 35.55 ± 1.12 per 100 μm^2) restored the number of "type 1" mitochondria in rotenone-induced PD mice (23.32 ± 1.60 per 100 μm^2) and prevented morphological changes (Fig. 3b). The average numbers of "type 1" and "type 2" mitochondria per 100 μm^2 in the control group were 42.68 ± 3.25 and 2.77 ± 0.18, respectively.

As PGC-1α and transcription factor A (TFAM) are key activators of mitochondrial gene transcription, the mRNA and protein levels of PGC-1α and TFAM in the midbrain and cortex were determined after PQQ treatment. Rotenone-induced injury decreased the mRNA level of TFAM in the cortex and midbrain to 66.18% ± 2.57% and 71.20% ± 4.70% of that in the control group, respectively (Fig. 4a, b). High-dose PQQ treatment upregulated the expression of TFAM in the cortex and midbrain to 128.5% ± 11.18% and 101.7% ± 10.79% of that in the control group, respectively (Fig. 4a, b). Although there was no significant change in the mRNA expression of PGC-1α in either the midbrain or cortex (data not shown), the protein level of PGC-1α was increased by medium and high dosages of PQQ to 153.50% ± 5.25% and 160.20% ± 8.57% compared with that in the control group in the cortex and midbrain, respectively (Fig. 4c–f). The downregulation of TFAM protein expression by rotenone-induced injury (cortex, 76.19% ± 2.27%; midbrain, 71.03% ± 3.14%) was also rescued by treatment with PQQ at a high dosage (cortex, 121.5% ± 10.91%; midbrain, 92.08% ± 4.18%) (Fig. 4c, d, g and h). These data indicated that PQQ might have promoted mitochondrial biogenesis in the brains of rotenone-injured PD mice by upregulating PGC-1α and TFAM expression.

Effect of PQQ on mitochondrial number in rotenone-injured SH-SY5Y cells

Our previous research suggested that 100 μM PQQ pretreatment for 24 h could inhibit the apoptosis of rotenone-injured SH-SY5Y cells and increase mitochondrial DNA (mtDNA) content. Here, we evaluated the effect of PQQ on mitochondria number by quantifying the intensity of MitoTracker® Green staining and the number of mitochondria in TEM images. MitoTracker® Green is a cell-permeable green fluorescent probe for mitochondrial labeling in live cells that localizes to mitochondria regardless of the mitochondrial membrane potential. Images following MitoTracker® Green staining showed that rotenone-induced injury dramatically decreased the fluorescence intensity (control, 0.0391 ± 0.0039; Rot, 0.0154 ± 0.0032), while an increase in fluorescence intensity was observed by treatment with PQQ at a dose of 100 μM (0.0342 ± 0.0052) (Fig. 5a). Pathological mitochondria were observed with rotenone-induced injury in SH-SY5Y cells, but this effect was mostly eliminated by PQQ treatment (Fig. 5b). In addition, decreases in the numbers of total (control, 57.30 ± 6.16 per 100 μm^2; Rot, 25.60 ± 1.33 per 100 μm^2) and "type 1" mitochondria (control, 54 ± 5.97 per 100 μm^2; Rot, 12.70 ± 1.56 per 100 μm^2) were also inhibited by 10 μM PQQ (total, 39.90 ± 1.45 per 100 μm^2; "type 1", 31.90 ± 1.22 per 100 μm^2) and 100 μM PQQ (total, 44.50 ± 2.36 per 100 μm^2; "type 1", 38.20 ± 2.19 per 100 μm^2) (Fig. 5c). The

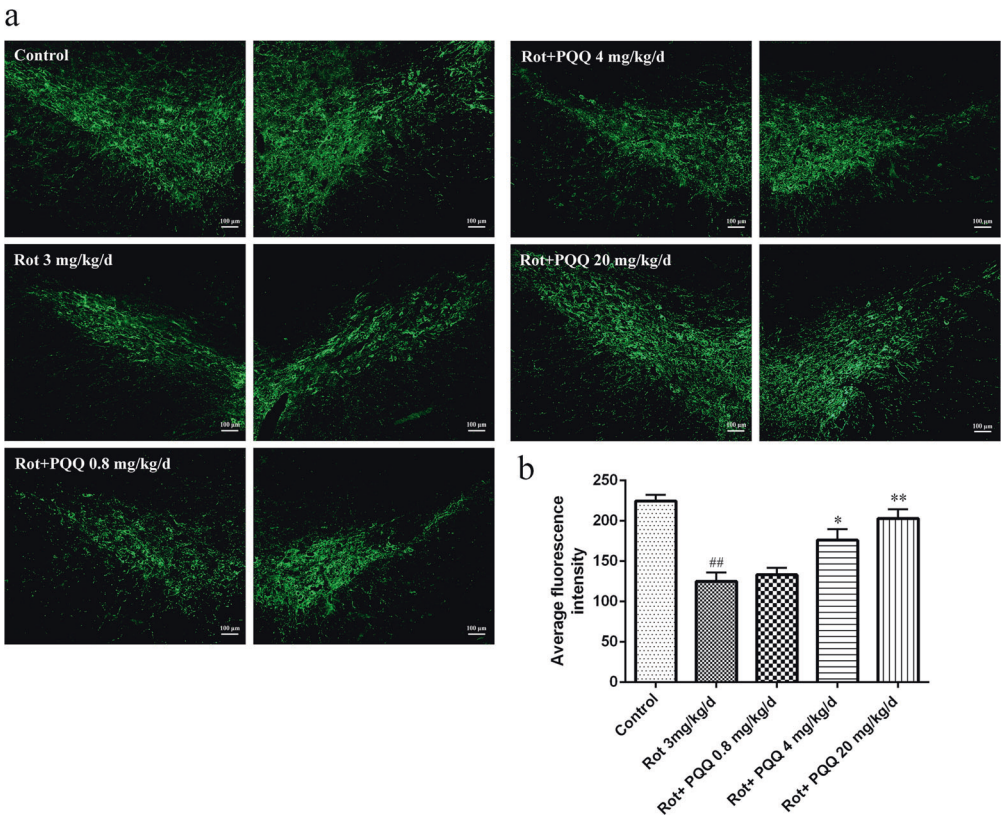

Fig. 2 PQQ prevented rotenone-induced neuronal loss in the SNpc of mice. a Representative images of TH immunostaining (green) in the SNpc. Scale bar = 100 μm. **b** Quantitative analysis of the fluorescence intensity in the SNpc. *$P < 0.05$ and **$P < 0.01$ vs the Rot group. ##$P < 0.01$ vs the control group ($n = 4$).

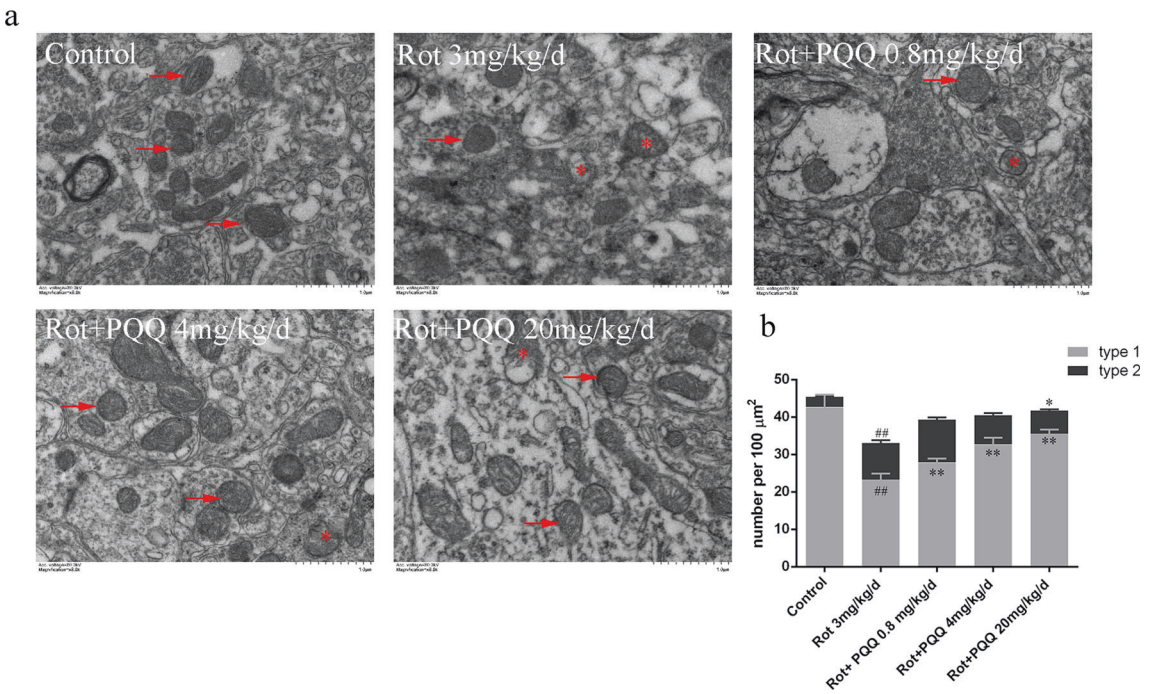

Fig. 3 PQQ affected the content and morphology of mitochondria in midbrains of PD mice. a Representative TEM images of mitochondria in the midbrains of PD mice with different treatments. Arrows indicate "type 1" mitochondria. Asterisks indicate "type 2" mitochondria. Scale bar = 1 μm. **b** Quantitative analysis of the average number of "type 1" and "type 2" mitochondria per 100 square micrometers (μm^2). *$P < 0.05$ and **$P < 0.01$ vs the Rot group. ##$P < 0.01$ vs the control group ($n = 20$).

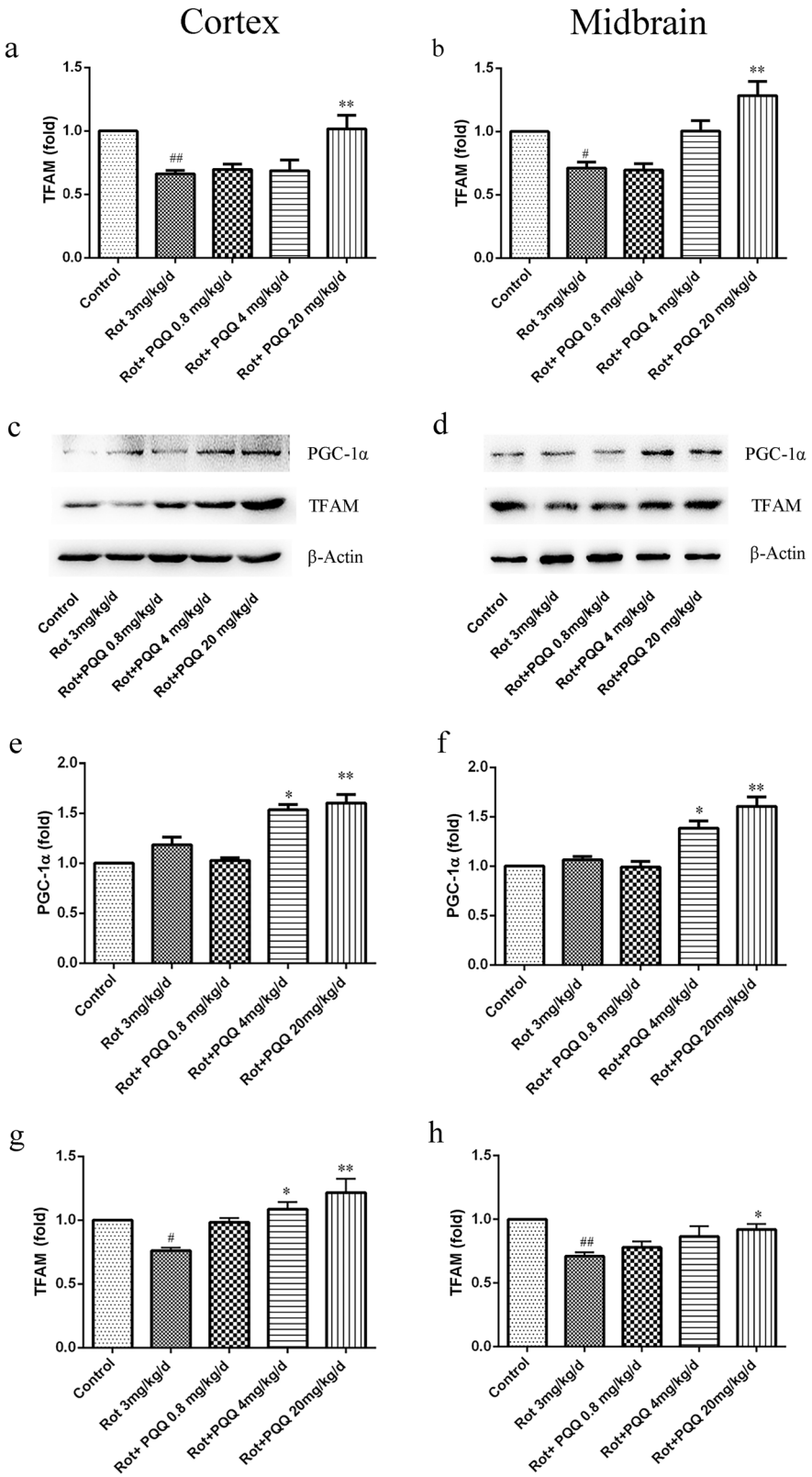

Fig. 4 PQQ regulated the expression of mitochondrial biogenesis-related genes and proteins in PD mice. a, **b** The mRNA expression of TFAM in the cortex (**a**) and midbrain (**b**) was measured. All data are expressed as the ratio compared with the control group. $^{**}P < 0.01$ vs the Rot group. $^{\#}P < 0.05$ and $^{\#\#}P < 0.01$ vs the control group ($n = 3$). **c**, **d** Representative Western blotting images of PGC-1α and TFAM protein expression in the cortex and midbrain of PD mice with different treatments. β-Actin served as a loading control. **e**, **f** The protein expression of PGC-1α in the cortex and midbrain is expressed as the ratio compared with the control group. **g**, **h** The protein expression of TFAM in the cortex and midbrain is expressed as the ratio compared with the control group. $^{*}P < 0.05$ and $^{**}P < 0.01$ vs the Rot group. $^{\#}P < 0.05$ and $^{\#\#}P < 0.01$ vs the control group ($n = 3$).

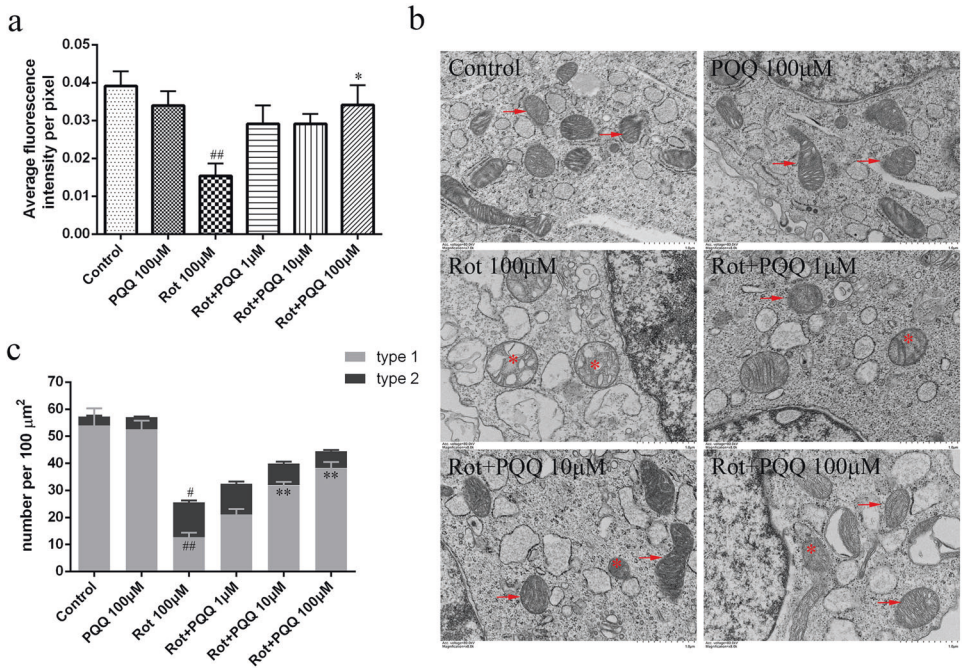

Fig. 5 PQQ promoted mitochondrial biogenesis in rotenone-injured SH-SY5Y cells. SH-SY5Y cells were plated in a 24-well plate and treated with rotenone or rotenone with different concentrations of PQQ. **a** Average fluorescence intensity per pixel in cultured SH-SY5Y cells after different treatments as indicated was measured by MitoTracker® Green staining. $^{*}P < 0.05$ vs the Rot group and $^{\#\#}P < 0.01$ vs the control group (no treatment) ($n = 10$). **b** Representative TEM images of mitochondria in SH-SY5Y cells with different treatments. Arrows indicate "type 1" mitochondria. Asterisks indicate "type 2" mitochondria. Scale bar = 1 μm. **c** Quantitative analysis of the average numbers of "type 1" and "type 2" mitochondria per 100 μm^2. $^{**}P < 0.01$ vs the Rot group. $^{\#}P < 0.05$, $^{\#\#}P < 0.01$ vs the control group ($n = 20$).

above data indicated that PQQ could rescue the decreased mitochondrial number induced by rotenone injury.

Effect of PQQ on protein phosphorylation in rotenone-injured SH-SY5Y cells

To further investigate the signaling pathways involved in the neuroprotective effect of PQQ, a rotenone-induced SH-SY5Y cell model was applied, and an antibody-based proteomic analysis was performed. Our previous studies suggested that 100 μM PQQ could restore mitochondrial dysfunction and inhibit cell apoptosis in rotenone-injured SH-SY5Y cells and midbrain dopaminergic neurons [11]. In this study, rotenone-injured SH-SY5Y cells were treated with or without 100 μM PQQ for 30 min, harvested, digested, and immunoprecipitated with PTMScan Direct reagents. Overall, 394 phosphosites and 260 phosphopeptides on 231 phosphoproteins were detected (Fig. 6a), covering 10 signaling pathways, including the AMPK signaling, adherens junction and Jak-STAT pathways (Fig. 6b). Thirty-three phosphosites displayed a statistically significant difference in expression (±2-fold, $P < 0.05$) between rotenone-injured cells and rotenone-injured cells treated with PQQ, and among these phosphosites, 4 phosphosites were upregulated, and 29 phosphosites were downregulated. A full list of the phosphoproteins identified as differentially expressed between the two groups is available in Table 2, and a Venn diagram is shown in Fig. 6c. Gene ontology (GO) analysis revealed that these proteins are mainly involved in the biological processes related to the regulation of neuronal cell death and apoptosis, wound healing, peptide biosynthesis, and metabolic processes (Fig. 6d). To further explore the impact of these differentially expressed phosphoproteins and discover internal connections between them, Kyoto Encyclopedia of Genes and Genomes (KEGG) enrichment analysis was performed, and the data indicated that the neurotrophin pathway, axon guidance and cAMP pathway were affected (Fig. 6e). A protein–protein interaction (PPI) network was also generated. The network consisted of a number of interconnected differentially expressed phosphoproteins, including 5′-AMP-activated protein kinase catalytic subunit alpha-1 (PRKAA1, also known as AMPKα1), Histone H2B (HIST1H2BI), focal adhesion kinase 1 (PTK2), Abl interactor 2 (ABI2), vesicle-associated membrane protein 8 (VAMP8), phosphoinositide phospholipase C (PLCG1), Kin of IRRE-like protein 1 (KIRREL), putative uncharacterized protein (NCK2), Rho-related GTP-binding protein (RhoC), and mammalian target of rapamycin (mTOR) (Fig. 6f).

AMPK phosphorylation was upregulated by PQQ in rotenone-injured SH-SY5Y cells and PD mice

PTMScan analysis showed that AMPK phosphorylation was significantly upregulated by PQQ in rotenone-injured cells. We used Western blotting to validate the results of the proteomic approach. The expression of phosphorylated AMPK was not affected by PQQ treatment in normal cells. AMPK phosphorylation was upregulated by 100 μM PQQ (1.80 ± 0.08) compared with that in the rotenone group (1.33 ± 0.05) (Fig. 7a, b), confirming that the AMPK pathway was activated by PQQ in rotenone-injured cells.

Then, we observed AMPK activation in PD mice. In the control group, phosphorylated AMPK levels did not change much over the drug administration period (1.00 ± 0.21 before injection and 1.10 ± 0.16, 1.03 ± 0.20, and 0.89 ± 0.10 at the end of weeks 1, 2, and 3 after the first injection, respectively). A slight increase in phosphorylated AMPK in the rotenone group (1.46 ± 0.18) at 1 week was detected. However, the activation of AMPK decreased to 1.23 ± 0.15 and 0.95 ± 0.18 after 2 and 3 weeks, respectively. PQQ at a high dosage significantly promoted the activation of AMPK by phosphorylation compared with that in the rotenone group over the whole process (1.93 ± 0.28, 1.60 ± 0.20, and 1.43 ± 0.24 at weeks 1, 2, and 3, respectively) (Fig. 7c, d). In vitro and

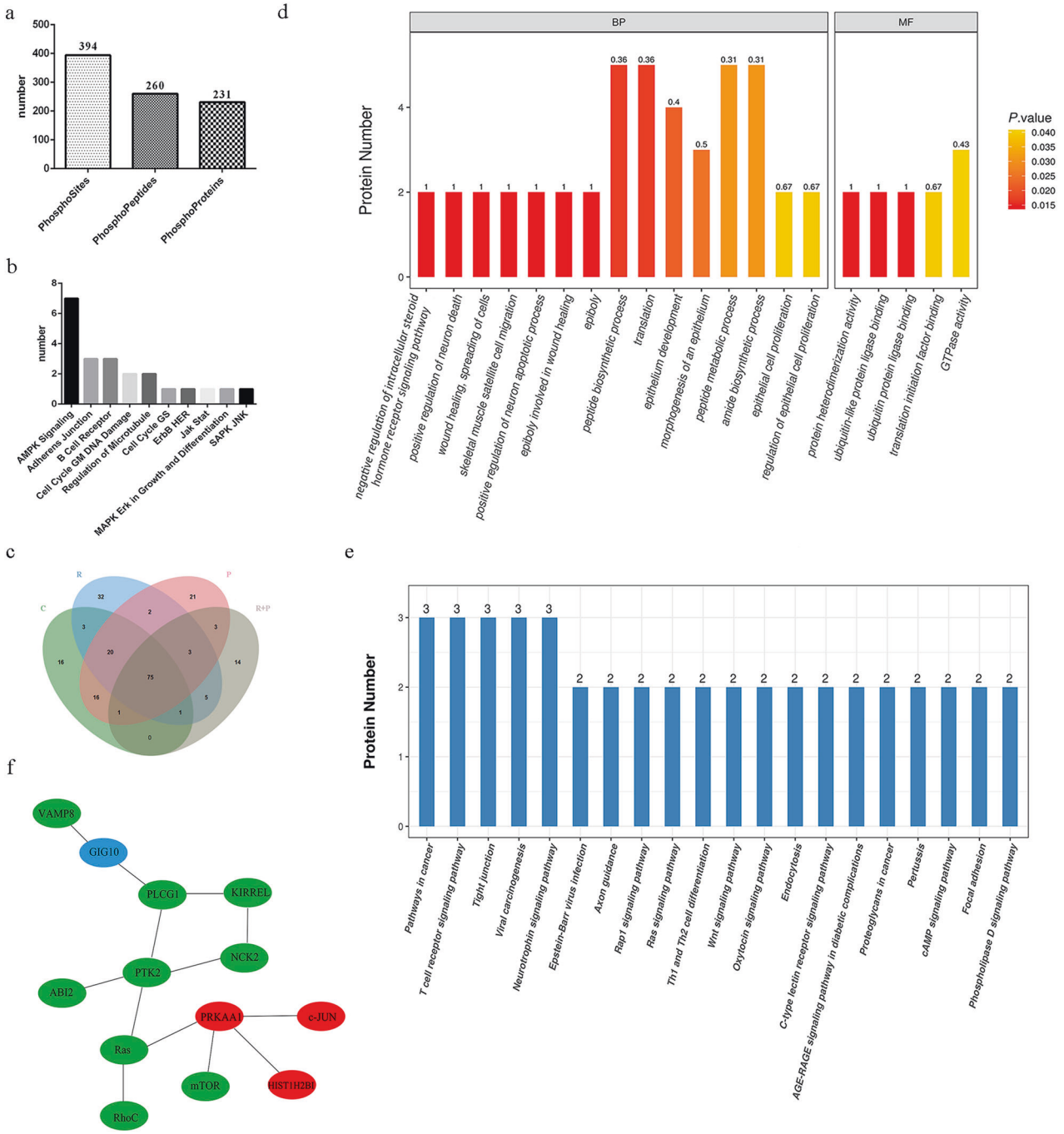

Fig. 6 PQQ changed the proteomic phosphorylation profile of rotenone-injured SH-SY5Y cells. SH-SY5Y cells were divided into four groups: the control group (no rotenone or PQQ), PQQ group (100 μM PQQ), Rotenone group (100 μM rotenone), PQQ + Rotenone group (100 μM PQQ + 100 μM rotenone). After 30 min of incubation, the cells were harvested for PTMScan multipathway analysis. **a** The total numbers of phosphosites, phosphopeptides and phosphoproteins detected in the experiment. **b** The number of proteins detected in different signal pathways. The AMPK signaling pathway was the most affected pathway. **c** Venn diagram showing the number of overlapping phosphopeptide sites in the control group (C), Rotenone group (R), PQQ group (P), and PQQ + Rotenone group (R+P). **d** GO enrichment analysis of phosphorylated proteins. The top 20 most differentially expressed phosphoproteins between the Rotenone and PQQ + Rotenone groups were classified depending on biological process (BP) and molecular function (MF). **e** KEGG enrichment analysis showing the pathways most significantly affected by PQQ treatment. **f** Protein–protein interaction (PPI) network analysis of differentially expressed phosphoproteins. Upregulated proteins are highlighted in red, and downregulated proteins are highlighted in green. PRKAA1, 5′-AMP-activated protein kinase catalytic subunit alpha-1; HIST1H2BI, Histone H2B; PTK2, focal adhesion kinase 1; ABI2, Abl interactor 2; VAMP8, vesicle-associated membrane protein 8; PLCG1, phosphoinositide phospholipase C; KIRREL, Kin of IRRE-like protein 1; NCK2, putative uncharacterized protein; RhoC, Rho-related GTP-binding protein; mTOR, mammalian target of rapamycin.

Table 2. Differentially expressed phosphoproteins between Rot and Rot + PQQ group.

Protein name	Gene name	Position	Amino acid	R + P/R[a]
5′-AMP-activated protein kinase catalytic subunit alpha-1	*PRKAA1*	183	T	2.50002
cDNA FLJ52549, highly similar to *L*-lactate dehydrogenase A chain (EC 1.1.1.27)		10	Y	+/−[b]
Transcription factor AP-1	*JUN*	63	S	+/−
Histone H2B	*HIST1H2BI*	65	S	+/−
Cyclin-dependent kinase 3 (Fragment)	*CDK3*	15	Y	0.488851
Serine/threonine-protein kinase mTOR (Fragment)	*MTOR*	104	S	0.42475
Cyclin-dependent kinase 14	*CDK14*	24	S	0.402758
Kin of IRRE-like protein 1	*KIRREL*	603	T	0.395268
40S ribosomal protein S6	*RPS6*	240	S	0.375106
Putative uncharacterized protein NCK2 (Fragment)	*NCK2*	50	Y	0.308865
Signal transducer and activator of transcription (Fragment)		700	Y	0.233678
Cell division cycle 2, G1 to S and G2 to M, isoform CRA_a	*CDC2*	15	Y	−/+
Ras homolog gene family, member A, isoform CRA_a	*RHOA*	34	Y	−/+
cDNA, FLJ92036, highly similar to Homo sapiens ribosomal protein L31 (RPL31), mRNA		108	Y	−/+
Histone H2B	*HIST1H2BI*	41	Y	−/+
Eukaryotic translation initiation factor 3 subunit B	*EIF3B*	662	S	−/+
cDNA FLJ56252, highly similar to Lethal(2) giant larvae protein homolog 2		280	S	−/+
WD repeat-containing protein 37 (Fragment)	*WDR37*	86	S	−/+
Vesicle-associated membrane protein 8	*VAMP8*	28	T	−/+
CLIP-associating protein 2	*CLASP2*	525	S	−/+
Focal adhesion kinase 1	*PTK2*	620	Y	−/+
Sodium-coupled neutral amino acid transporter 2	*SLC38A2*	41	Y	−/+
Abl interactor 2 (Fragment)	*ABI2*	79	Y	−/+
Tight junction protein ZO-3 (Fragment)	*TJP3*	98	T	−/+
Tubulin alpha-1B chain	*TUBA1B*	223	T	−/+
Phosphoinositide phospholipase C (Fragment)	*PLCG1*	905	Y	−/+
GIG10		108	S	−/+
Rho-related GTP-binding protein RhoC (Fragment)	*RHOC*	34	Y	−/+
La-related protein 1	*LARP1*	631	S	−/+
La-related protein 1	*LARP1*	627	S	−/+
cDNA FLJ40872 fis, clone TUTER2000283, highly similar to Homo sapiens transformer-2-beta (SFRS10)		230	S	−/+
cDNA FLJ40872 fis, clone TUTER2000283, highly similar to Homo sapiens transformer-2-beta (SFRS10)		228	S	−/+
Prohibitin-2	*PHB2*	121	Y	−/+

[a]R + P/R = the ratio of average abundance in Rot + PQQ group/Rot group.
[b]+ = detectable; − = do not detectable.

in vivo data suggested that PQQ could increase AMPK activation in both rotenone-injured cells and rotenone-injured PD mice.

AMPK activation is required for the protective effect of PQQ in rotenone-injured SH-SY5Y cells

Dorsomorphin (compound C) 2HCl is a potent, reversible, selective AMPK inhibitor. We first demonstrated by Western blotting that dorsomorphin at 4 μM significantly inhibited the expression of PGC-1α, a downstream molecule of AMPK, in SH-SY5Y cells after rotenone injury with or without PQQ treatment (control, 1.00 ± 0.09; dorsomorphin, 1.00 ± 0.05; Rot, 0.41 ± 0.03; Rot+dorsomorphin, 0.54 ± 0.04; Rot+PQQ, 0.80 ± 0.04; Rot+PQQ + dorsomorphin, 0.57 ± 0.04) (Fig. 8a, b). The increased cell viability in rotenone-injured SH-SY5Y cells treated with PQQ was inhibited by dorsomorphin pretreatment (control, 0.92 ± 0.03; dorsomorphin, 0.86 ± 0.02; Rot, 0.58 ± 0.02; Rot+dorsomorphin, 0.56 ± 0.01; Rot+PQQ, 0.76 ± 0.02; Rot+PQQ + dorsomorphin, 0.60 ± 0.02) (Fig. 8c), suggesting that the inactivation of AMPK could reduce the neuroprotective effect of PQQ.

The average fluorescence intensity of MitoTracker® Green staining showed that inhibition of AMPK activation by dorsomorphin attenuated the increase in mitochondrial number due to PQQ pretreatment in rotenone-injured SH-SY5Y cells (control, 0.0400 ± 0.0037; dorsomorphin, 0.0360 ± 0.0025; Rot, 0.0180 ± 0.0023; Rot+dorsomorphin, 0.0148 ± 0.0015; Rot+PQQ, 0.0300 ± 0.0020; Rot+PQQ + dorsomorphin, 0.0192 ± 0.0203) (Fig. 9b, c). The mtDNA content quantified by qRT-PCR also indicated that AMPK inhibition reduced the mitochondrial mass (0.46 ± 0.04) compared with that in the PQQ treatment group (0.68 ± 0.04) (Fig. 9d).

Moreover, TEM observation showed that the inactivation of AMPK significantly decreased the number of total and "type 1" mitochondria (total, 23.90 ± 1.06; "type 1", 16.00 ± 0.82) in SH-SY5Y cells compared with those in the PQQ treatment group (total, 35.20 ± 2.12; "type 1", 28.70 ± 1.88) (Fig. 9e, f). Together, these results demonstrated that activation of the AMPK signaling pathway might be involved in the regulation of mitochondrial biogenesis by PQQ in rotenone-injured SH-SY5Y cells.

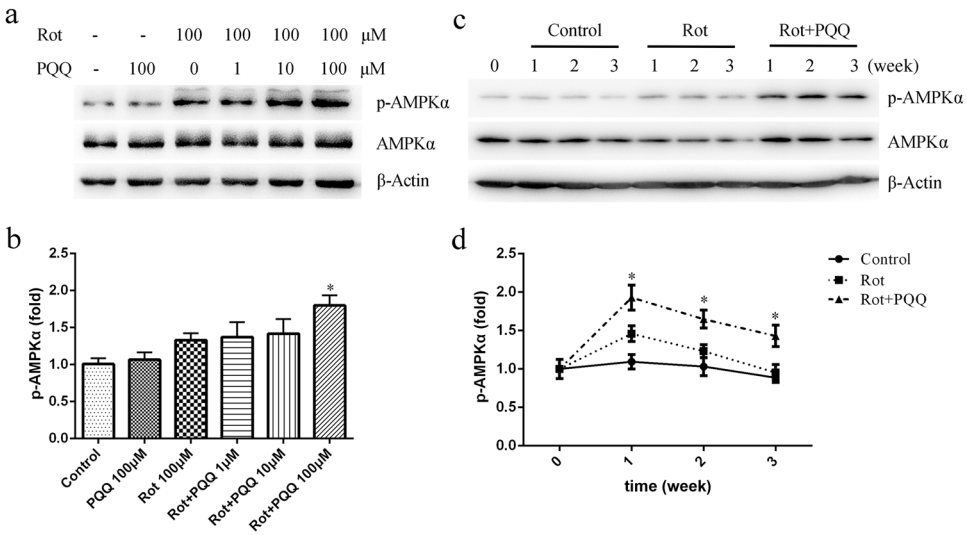

Fig. 7 Western blotting validation of PQQ-induced activation of AMPK signaling in rotenone-injured SH-SY5Y cells and rotenone-injured PD mice. a SH-SY5Y cells were treated with rotenone or rotenone with different concentrations of PQQ for 30 min, after which both phosphorylated AMPKα and total AMPKα were detected by Western blotting analysis. β-Actin served as the internal control. **b** Quantification of the relative expression of phosphorylated AMPKα compared with that in the control group. The ratio of phosphorylated AMPK (p-AMPKα) to total AMPKα in the control group was set as "1". $^*P < 0.05$ vs the Rot group ($n = 3$). **c** Rotenone (3 mg·kg^{-1}·d^{-1}) was intraperitoneally administered once daily for 3 weeks. PQQ at a high dosage (20 mg·kg^{-1}·d^{-1}) was intraperitoneally administered immediately after rotenone injection. The control group was injected with normal saline containing 2% DMSO. The midbrains were harvested at the end of weeks 1, 2, and 3 for Western blotting analysis. β-Actin served as the internal control. **d** Quantification of the relative expression of p-AMPKα. The ratio of p-AMPKα to total AMPKα in the control group before drug administration was set as "1". $^*P < 0.05$ vs the Rot group ($n = 4$).

DISCUSSION

The pathogenesis of PD is multifactorial and associated with mitochondrial dysfunction, oxidative stress, apoptosis, and inflammation [2]. Although the exact mechanisms underlying PD progression have not been well elucidated, natural products and bioactive compounds with multiple targets in the central nervous system seem to be more effective and safer for PD treatment than single-target compounds [22]. PQQ is a redox cofactor found in soil, foods such as kiwifruit, and human breast milk [23]. Recent research indicates that PQQ protects against oxidative stress damage, apoptosis, and mitochondrial dysfunction [24, 25]. In the present study, we reported that PQQ protected rotenone-induced PD mice and rotenone-injured SH-SY5Y cells by promoting mitochondrial biogenesis. The AMPK signaling pathway was activated by PQQ, which was required for the protective effects of PQQ in PD models.

Bioactive compounds with the ability to stimulate mitochondrial biogenesis are thought to improve health by promoting energy utilization, protecting against reactive oxygen species and inhibiting apoptosis [26]. PQQ was reported to protect cells from autophagy-dependent apoptosis induced by doxorubicin via the lysosomal-mitochondrial axis [27]. PQQ could also exert protective effects against oxidative stress damage and apoptosis in a diabetic nephropathy model in vitro. These protective effects were associated with increased antioxidants and inhibited ROS production, which required activation of the PI3K/Akt signaling pathway [28]. Our previous study indicated that PQQ could prevent mitochondrial dysfunction in PD rats in which rotenone was injected into the medial forebrain bundle (MFB) [8]. However, this PD model established by the MFB injection of rotenone is not completely consistent with the slow progression of PD. In this study, we established a mouse PD model by intraperitoneal injection of rotenone and then investigated the neuroprotective effect and underlying mechanism of PQQ. As expected, intraperitoneal rotenone injection for 21 consecutive days induced motor function deficits and neuronal loss in the SNpc [29]. Bradykinesia and locomotor activity dysfunction were observed in a rat PD model induced by intraperitoneal injection of rotenone [30]. Here, we demonstrated that PQQ could prevent motor deficits and reduce the loss of dopaminergic neurons in the SNpc in a dose-dependent manner. As neurological dysfunctions in PD patients and in animal models are related to dopaminergic neuronal loss in the SNpc and the depletion of dopamine in the striatum, our data indicated that PQQ exerted a protective effect in PD mice by inhibiting neuronal loss, thus reducing locomotor dysfunctions.

Mitochondrial function is primarily maintained by mitochondrial quality control mechanisms, including mitochondrial biogenesis, mitochondrial fission and fusion, and mitochondrial autophagy [31]. Mitochondrial biogenesis is thought to be regulated by the PGC-1α network, while the Nrf2/ARE signaling cascade is involved in mitochondrial biogenesis [32, 33]. PQQ supplementation could upregulate the molecular signaling responses indicative of mitochondrial biogenesis within skeletal muscle [34]. In cultured mouse hepatocytes, PQQ exposure could promote the phosphorylation of CREB and the expression of PGC-1α, thus increasing the mtDNA content [26]. We also found that PQQ could maintain mitochondrial physiological functions and promote the expression and translocation of Nrf2 in glutamate-damaged hippocampal neurons [35], suggesting that PQQ exerts a neuroprotective effect by promoting mitochondrial biogenesis. In this study, we observed that the number of mitochondria with an integral structural was significantly increased with PQQ treatment both in vivo and in vitro, suggesting that PQQ might promote mitochondrial biogenesis in rotenone-induced PD models. As mitochondrial turnover by autophagy or proteolysis is important to eliminate defective mitochondria to maintain cellular homeostasis [36], mitochondrial degradation should also be considered in future studies.

As a transcriptional coactivator, PGC-1α plays a significant role in promoting mitochondrial biogenesis [37]. PGC-1α acts as a transcription factor for mitochondrial biogenesis by transactivating Nrf1/2 and increasing the expression of TFAM [38, 39]. TFAM, a mtDNA-binding protein that plays a central role in the mtDNA stress-induced inflammatory response, is necessary for mitochondrial genome maintenance [40]. Decreases in PGC-1α and its downstream genes were detected in the postmortem brains of PD

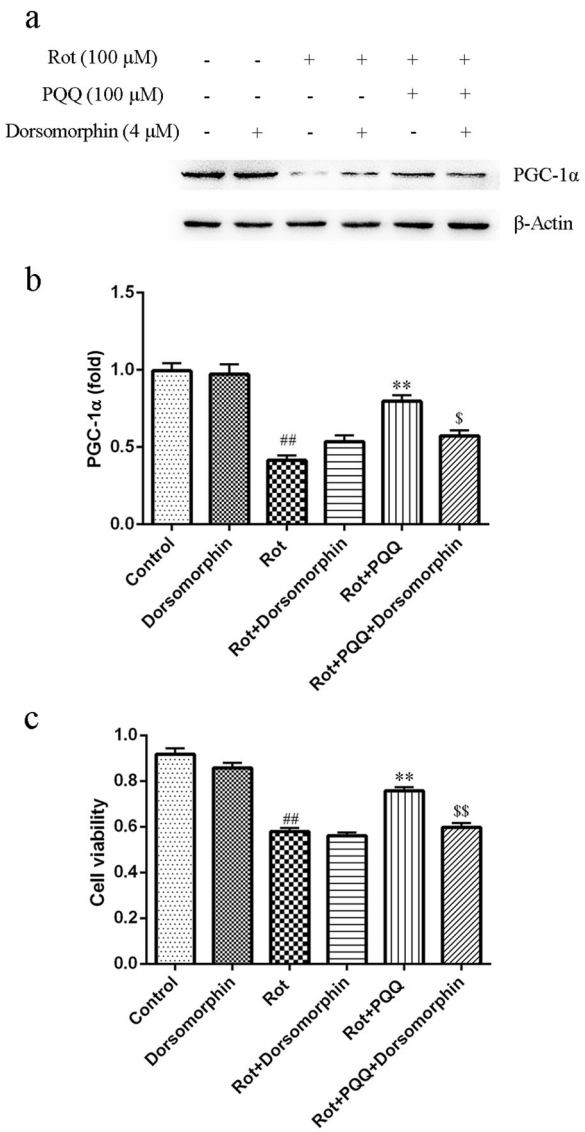

Fig. 8 Inhibition of AMPK by dorsomorphin (compound C) 2HCl eliminated the protective effect of PQQ in rotenone-injured SH-SY5Y cells. Dorsomorphin at a final concentration of 4 μM was added to SH-SY5Y cells 30 min prior to rotenone and PQQ treatment. Cellular proteins were extracted after PQQ treatment for 30 min and subjected to Western blotting analysis, and cell viability was measured after PQQ treatment for 24 h. **a** Representative images of PGC-1α detected by Western blotting analysis. β-Actin served as the internal control. **b** Quantification of the relative expression of PGC-1α. $^{**}P < 0.01$ vs the Rot group, $^{\#\#}P < 0.01$ vs the control group, $^{\$}P < 0.05$ vs the Rot+PQQ group ($n = 3$). **c** Cell viability was measured by CCK-8 assay, and the absorbance (optical density, *OD*) at 450 nm was measured by spectrophotometry. $^{**}P < 0.01$ vs the Rot group, $^{\#\#}P < 0.01$ vs the control group, $^{\$\$}P < 0.01$ vs the Rot + PQQ group ($n = 10$).

patients [41]. PGC-1α-knockout mice were found to be more sensitive to MPTP damage than control mice [42], and deletion of the Drosophila PGC-1α ortholog spargel in flies caused PD-like symptoms [43]. In contrast, activation of PGC-1α was sufficient to rescue the disease phenotypes of Parkin and LRRK2 genetic fly models of PD [43]. Activation or overexpression of PGC-1α caused an increase in the expression of nuclear-encoded subunits of the mitochondrial respiratory chain and prevented the degeneration of dopaminergic neurons in cellular or animal models induced by mutant α-synuclein, rotenone, or MPTP [42]. Moreover, increased mitochondrial biogenesis caused by the stabilization of endogenous PGC-1α exerted a neuroprotective against mitochondrial insults [44]. This evidence suggests that targeting PGC-1α might be an effective strategy for neuroprotection in PD. Although we did not detect a significant change in PGC-1α mRNA in the cortex or midbrain of PD mice, which is not consistent with the data in SH-SY5Y cells [8], we found that PQQ had a significant inhibitory effect on the decrease in PGC-1α and TFAM protein expression caused by rotenone injury in vivo. The effect of PQQ on protein expression, combined with the increase in mitochondrial number, indicated that PQQ might promote mitochondrial biogenesis by upregulating PGC-1α and TFAM.

To further analyze the signaling mechanisms involved in the neuroprotective effect of PQQ, rotenone-injured SH-SY5Y cells and PTMScan analysis coupled with LC-MS/MS methods were applied [45]. PTMs have emerged as important modulators of some important proteins in PD pathogenesis [14, 46]. Activation of LRRK2 by phosphorylation is thought to be one of the causes of PD, and an LRRK2 kinase inhibitor could protect cells against rotenone-induced noxious effects [15]. Among the differentially phosphorylated proteins upon PQQ treatment in our cell injury model, AMPK is a serine/threonine kinase that plays an important role in cellular energy homeostasis, mitochondrial biogenesis, and autophagy [47]. Induction of adaptive responses via the AMPK signaling pathway was shown to be important for the survival of human cells under oxidative stress induced by mitochondrial dysfunction [48]. AMPK was expected to be activated by rotenone injury, as previously reported. However, AMPK activation was observed after incubation with rotenone for 24 h [49, 50]. In our experiment, rotenone was applied for only 30 min, and only weak activation of AMPK was observed in the rotenone group. In the PD mice, AMPK activation was observed after 1 week, and phosphorylated AMPK levels then decreased to normal as dopaminergic neuronal loss occurred. Consistent with the PTMScan data, we confirmed that PQQ could activate AMPK phosphorylation in both rotenone-injured cells and rotenone-injured PD mice.

Activation of the AMPK signaling pathway was reported to enhance mitochondrial biogenesis and energy bioavailability by regulating PGC-1α and TFAM [51]. Our previous study proved that the expression of PGC-1α and TFAM in rotenone-injured SH-SY5Y cells could be upregulated by PQQ [8]. Here, we also observed an increase in PGC-1α and TFAM in PD mice. Thus, we deduce that the upregulation of these transcription factors is related to activation of the AMPK signaling pathway. Activation of AMPK enhanced the expression of PGC-1α by p38MAPK signaling in cancer cells to induce mitochondrial biogenesis [52]. In skeletal muscle cells, AMPK upregulated PGC-1α expression by increasing PGC-1α promoter activity or the direct phosphorylation of PGC-1α [53, 54]. However, whether AMPK can upregulate the expression of PGC-1α in neuronal cells through the above pathways has not been confirmed.

Our data showed that inhibition of AMPK by dorsomorphin reduced the upregulation of PGC-1α induced by PQQ and eliminated the protective effect of PQQ in rotenone-injured SH-SY5Y cells. Mitochondria number and the mtDNA content were also regulated by AMPK inhibition, suggesting that the activation of AMPK was required for the regulation of mitochondrial biogenesis by PQQ. Dorsomorphin is a potent, reversible, selective AMPK inhibitor [55, 56]. Inhibition of AMPK activity by dorsomorphin was reported to almost completely inhibit autophagic proteolysis in HT-29 cells [57], while autophagy induction might have exerted protective effects in rotenone-injured cells [29, 58]. Whether PQQ can induce autophagy by AMPK activation and then display neuroprotective effects needs further investigation.

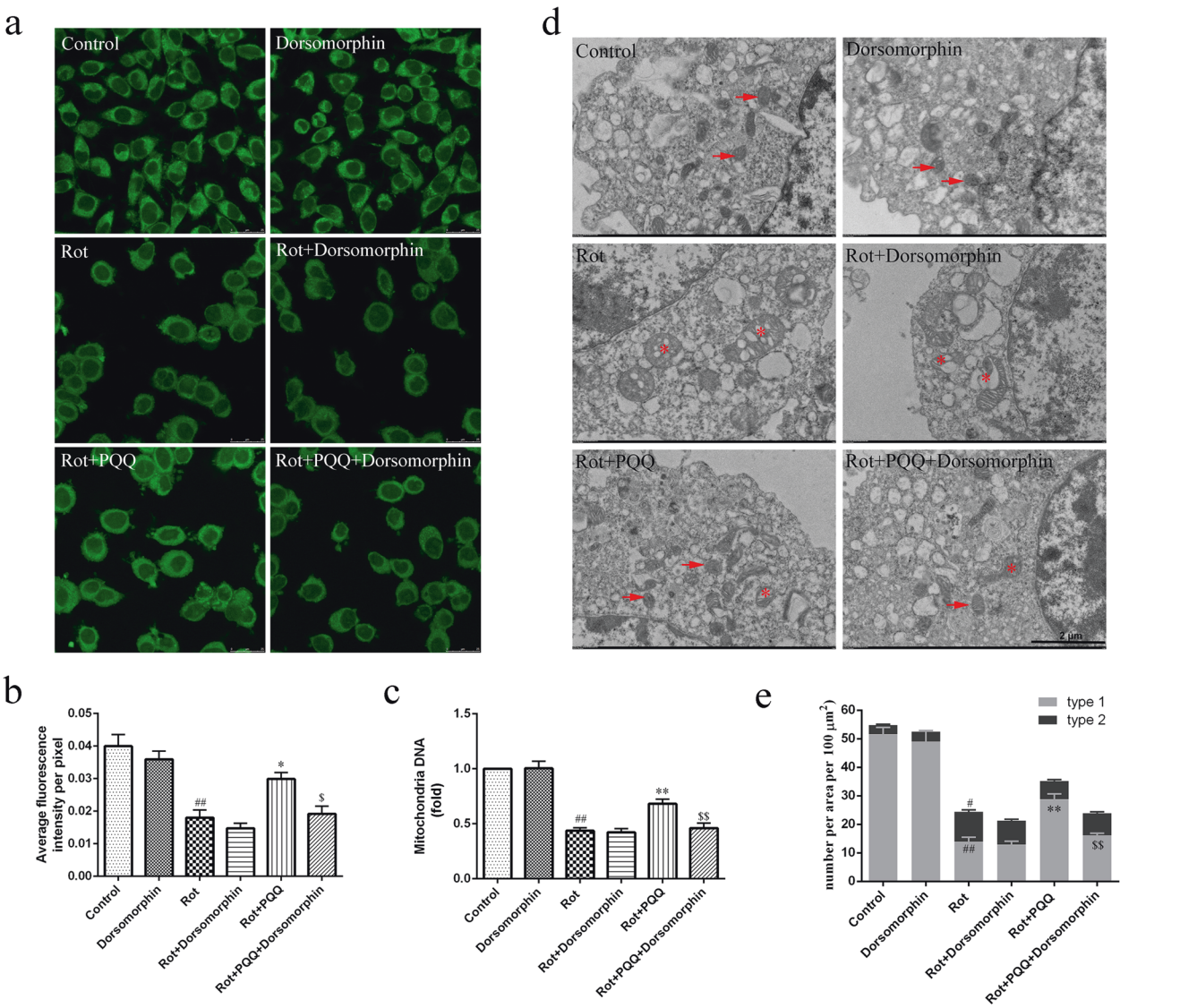

Fig. 9 Inhibition of AMPK by dorsomorphin (compound C) 2HCl attenuated mitochondrial biogenesis induced by PQQ in rotenone-injured SH-SY5Y cells. Dorsomorphin at a final concentration of 4 μM was added to SH-SY5Y cells 30 min prior to rotenone and PQQ treatment. **a** MitoTracker® Green staining of SH-SY5Y cells was performed 24 h after PQQ treatment (scale bar = 25 μm). **b** Average fluorescence intensity per pixel in cultured SH-SY5Y cells after different treatments as indicated was measured by MitoTracker® Green staining. $^{*}P < 0.05$ vs the Rot group, $^{\#\#}P < 0.01$ vs the control group, $^{\$}P < 0.05$ vs the Rot + PQQ group ($n = 10$). **c** Mitochondrial DNA content was measured by real-time PCR of cultured SH-SY5Y cells after the indicated treatments. $^{**}P < 0.01$ vs the Rot group. $^{\#\#}P < 0.01$ vs the control group, $^{\$\$}P < 0.01$ vs the Rot + PQQ group ($n = 10$). **d** Representative TEM images of SH-SY5Y cells treated with dorsomorphin. Arrows indicate "type 1" mitochondria. Asterisks indicate "type 2" mitochondria. Scale bar = 2 μm. **e** Quantitative analysis of the average number of "type 1" and "type 2" mitochondria per 100 μm^2. $^{**}P < 0.01$ vs the Rot group. $^{\#}P < 0.05$, $^{\#\#}P < 0.01$ vs the control group, $^{\$\$}P < 0.01$ vs the Rot + PQQ group ($n = 20$).

CONCLUSION

Taken together, the results of this study demonstrated that PQQ could improve motor functions, reduce the loss of midbrain dopaminergic neurons, and promote mitochondrial biogenesis in rotenone-induced PD mice, showing a neuroprotective effect. Activation of the AMPK signaling pathway by PQQ might be involved in the regulation of mitochondrial biogenesis and was responsible for the protective effect of PQQ in rotenone-injured SH-SY5Y cells.

ACKNOWLEDGEMENTS

This study was supported by the National Key Research and Development Program of China (Grant No. 2017YFA0104700), National Natural Science Foundation of China (81771404), the Natural Science Foundation of Jiangsu Province (Grant No. BK20161285), the Priority Academic Program Development of Jiangsu Higher Education Institutions (PAPD), Jiangsu Provincial Key Medical Center, and Jiangsu Students' innovation and entrepreneurship training program (Grant No. 201810304096X).

AUTHOR CONTRIBUTIONS

QC and JC carried out the cell culture, qPCR, and Western blotting experiments. HG, JLL, and JZ carried out the animal model and behavior tests. XYG, YS, and YZ carried out the TH staining. SY and QZ carried out the PTMscan analysis and TEM observation. QZ and QC analyzed the data and wrote the paper. FD edited the paper. QZ and FD designed the study and supervised the research.

ADDITIONAL INFORMATION

Competing interests: The authors declare no competing interests.

REFERENCES

1. Raza C, Anjum R, Shakeel NUA. Parkinson's disease: mechanisms, translational models and management strategies. Life Sci. 2019;226:77–90.
2. Poewe W, Seppi K, Tanner CM, Halliday GM, Brundin P, Volkmann J, et al. Parkinson disease. Nat Rev Dis Prim. 2017;3:17013.
3. Tang BL. Sirt1 and the mitochondria. Mol Cells. 2016;39:87–95.
4. Fernandez-Moriano C, Gonzalez-Burgos E, Gomez-Serranillos MP. Mitochondria-targeted protective compounds in Parkinson's and Alzheimer's diseases. Oxid Med Cell Longev. 2015;2015:408927.
5. Cannon JR, Tapias V, Na HM, Honick AS, Drolet RE, Greenamyre JT. A highly reproducible rotenone model of Parkinson's disease. Neurobiol Dis. 2009;34:279–90.
6. Johnson ME, Bobrovskaya L. An update on the rotenone models of Parkinson's disease: their ability to reproduce the features of clinical disease and model gene-environment interactions. Neurotoxicology. 2015;46:101–16.
7. Tabata Y, Imaizumi Y, Sugawara M, Andoh-Noda T, Banno S, Chai M, et al. T-type calcium channels determine the vulnerability of dopaminergic neurons to mitochondrial stress in familial Parkinson disease. Stem Cell Rep. 2018;11:1171–84.
8. Lu J, Chen S, Shen M, He Q, Zhang Y, Shi Y, et al. Mitochondrial regulation by pyrroloquinoline quinone prevents rotenone-induced neurotoxicity in Parkinson's disease models. Neurosci Lett. 2018;687:104–10.
9. Zhang ZN, Zhang JS, Xiang J, Yu ZH, Zhang W, Cai M, et al. Subcutaneous rotenone rat model of Parkinson's disease: dose exploration study. Brain Res. 2017;1655:104–13.
10. Park JS, Davis RL, Sue CM. Mitochondrial dysfunction in Parkinson's disease: new mechanistic insights and therapeutic perspectives. Curr Neurol Neurosci Rep. 2018;18:21.
11. Zhang Q, Chen S, Yu S, Qin J, Zhang J, Cheng Q, et al. Neuroprotective effects of pyrroloquinoline quinone against rotenone injury in primary cultured midbrain neurons and in a rat model of Parkinson's disease. Neuropharmacology. 2016;108:238–51.
12. Zhang Q, Zhang J, Jiang C, Qin J, Ke K, Ding F. Involvement of ERK1/2 pathway in neuroprotective effects of pyrroloquinoline quinine against rotenone-induced SH-SY5Y cell injury. Neuroscience. 2014;270:183–91.
13. Qin J, Wu M, Yu S, Gao X, Zhang J, Dong X, et al. Pyrroloquinoline quinone-conferred neuroprotection in rotenone models of Parkinson's disease. Toxicol Lett. 2015;238:70–82.
14. Pajarillo E, Rizor A, Lee J, Aschner M, Lee E. The role of posttranslational modifications of alpha-synuclein and LRRK2 in Parkinson's disease: potential contributions of environmental factors. Biochim Biophys Acta Mol Basis Dis. 2019;1865:1992–2000.
15. Mendivil-Perez M, Velez-Pardo C, Jimenez-Del-Rio M. Neuroprotective effect of the LRRK2 kinase inhibitor PF-06447475 in human nerve-like differentiated cells exposed to oxidative stress stimuli: implications for Parkinson's disease. Neurochem Res. 2016;41:2675–92.
16. Zhang L, Hao J, Zheng Y, Su R, Liao Y, Gong X, et al. Fucoidan protects dopaminergic neurons by enhancing the mitochondrial function in a rotenone-induced rat model of Parkinson's disease. Aging Dis. 2018;9:590–604.
17. Liu K, Xu H, Xiang H, Sun P, Xie J. Protective effects of Ndfip1 on MPP^{+}-induced apoptosis in MES23.5 cells and its underlying mechanisms. Exp Neurol. 2015;273:215–24.
18. Stokes MP, Farnsworth CL, Moritz A, Silva JC, Jia X, Lee KA, et al. PTMScan direct: identification and quantification of peptides from critical signaling proteins by immunoaffinity enrichment coupled with LC-MS/MS. Mol Cell Proteom. 2012;11:187–201.
19. Stokes MP, Silva JC, Jia X, Lee KA, Polakiewicz RD, Comb MJ. Quantitative profiling of DNA damage and apoptotic pathways in UV damaged cells using PTMScan Direct. Int J Mol Sci. 2012;14:286–307.
20. Choi DY, Lee MK, Hong JT. Lack of CCR5 modifies glial phenotypes and population of the nigral dopaminergic neurons, but not MPTP-induced dopaminergic neurodegeneration. Neurobiol Dis. 2013;49:159–68.
21. Wang ES, Zhang XP, Yao HB, Wang G, Chen SW, Gao WW, et al. Tetranectin knockout mice develop features of Parkinson disease. Cell Physiol Biochem. 2014;34:277–87.
22. Calabresi P, Di Filippo M. Multitarget disease-modifying therapy in Parkinson's disease? Lancet Neurol. 2015;14:975–6.
23. Felton LM, Anthony C. Biochemistry: role of PQQ as a mammalian enzyme cofactor? Nature. 2005;433:E10. discussion E11-2.
24. Misra HS, Rajpurohit YS, Khairnar NP. Pyrroloquinoline-quinone and its versatile roles in biological processes. J Biosci. 2012;37:313–25.
25. Wen H, He Y, Zhang K, Yang X, Hao D, He B. Mini-review: Functions and action mechanisms of PQQ in osteoporosis and neuro injury. Curr Stem Cell Res Ther. 2020;15:32–6.
26. Chowanadisai W, Bauerly KA, Tchaparian E, Wong A, Cortopassi GA, Rucker RB. Pyrroloquinoline quinone stimulates mitochondrial biogenesis through cAMP response element-binding protein phosphorylation and increased PGC-1alpha expression. J Biol Chem. 2010;285:142–52.
27. Jiang C, Jiang L, Li Q, Liu X, Zhang T, Yang G, et al. Pyrroloquinoline quinine ameliorates doxorubicin-induced autophagy-dependent apoptosis via lysosomal-mitochondrial axis in vascular endothelial cells. Toxicology. 2019;425:152238.
28. Wang Z, Li Y, Wang Y, Zhao K, Chi Y, Wang B. Pyrroloquinoline quinine protects HK-2cells against high glucose-induced oxidative stress and apoptosis through Sirt3 and PI3K/Akt/FoxO3a signaling pathway. Biochem Biophys Res Commun. 2019;508:398–404.
29. Zhang Y, Guo H, Guo X, Ge D, Shi Y, Lu X, et al. Involvement of Akt/mTOR in the neurotoxicity of rotenone-induced Parkinson's disease models. Int J Environ Res Public Health. 2019;16:3811.
30. Valdez LB, Zaobornyj T, Bandez MJ, Lopez-Cepero JM, Boveris A, Navarro A. Complex I syndrome in striatum and frontal cortex in a rat model of Parkinson disease. Free Radic Biol Med. 2019;135:274–82.
31. Jiang X, Jin T, Zhang H, Miao J, Zhao X, Su Y, et al. Current progress of mitochondrial quality control pathways underlying the pathogenesis of Parkinson's disease. Oxid Med Cell Longev. 2019;2019:4578462.
32. Gureev AP, Shaforostova EA, Popov VN. Regulation of mitochondrial biogenesis as a way for active longevity: interaction between the Nrf2 and PGC-1alpha signaling pathways. Front Genet. 2019;10:435.
33. Scarpulla RC. Metabolic control of mitochondrial biogenesis through the PGC-1 family regulatory network. Biochim Biophys Acta. 2011;1813:1269–78.
34. Hwang P, Willoughby DS. Mechanisms behind pyrroloquinoline quinone supplementation on skeletal muscle mitochondrial biogenesis: possible synergistic effects with exercise. J Am Coll Nutr. 2018;37:738–48.
35. Zhang Q, Ding M, Cao Z, Zhang J, Ding F, Ke K. Pyrroloquinoline quinine protects rat brain cortex against acute glutamate-induced neurotoxicity. Neurochem Res. 2013;38:1661–71.
36. Diaz F, Moraes CT. Mitochondrial biogenesis and turnover. Cell Calcium. 2008;44:24–35.
37. Austin S, St-Pierre J. PGC1alpha and mitochondrial metabolism–emerging concepts and relevance in ageing and neurodegenerative disorders. J Cell Sci. 2012;125(Pt 21):4963–71.
38. Li PA, Hou X, Hao S. Mitochondrial biogenesis in neurodegeneration. J Neurosci Res. 2017;95:2025–9.
39. Ventura-Clapier R, Garnier A, Veksler V. Transcriptional control of mitochondrial biogenesis: the central role of PGC-1alpha. Cardiovasc Res. 2008;79:208–17.
40. Kang I, Chu CT, Kaufman BA. The mitochondrial transcription factor TFAM in neurodegeneration: emerging evidence and mechanisms. FEBS Lett. 2018;592:793–811.
41. Zheng B, Liao Z, Locascio JJ, Lesniak KA, Roderick SS, Watt ML, et al. PGC-1alpha, a potential therapeutic target for early intervention in Parkinson's disease. Sci Transl Med. 2010;2:52ra73.
42. Mudo G, Makela J, Di Liberto V, Tselykh TV, Olivieri M, Piepponen P, et al. Transgenic expression and activation of PGC-1alpha protect dopaminergic neurons in the MPTP mouse model of Parkinson's disease. Cell Mol Life Sci. 2012;69:1153–65.
43. Ng CH, Basil AH, Hang L, Tan R, Goh KL, O'Neill S, et al. Genetic or pharmacological activation of the Drosophila PGC-1alpha ortholog spargel rescues the disease phenotypes of genetic models of Parkinson's disease. Neurobiol Aging. 2017;55:33–7.
44. Hasegawa K, Yasuda T, Shiraishi C, Fujiwara K, Przedborski S, Mochizuki H, et al. Promotion of mitochondrial biogenesis by necdin protects neurons against mitochondrial insults. Nat Commun. 2016;7:10943.
45. Kato C, Kawai E, Shimizu N, Mikekado T, Kimura F, Miyazawa T, et al. Determination of pyrroloquinoline quinone by enzymatic and LC-MS/MS methods to clarify its levels in foods. PLoS One. 2018;13:e0209700.
46. Wang Y, Liu J, Chen M, Du T, Duan C, Gao G, et al. The novel mechanism of rotenone-induced alpha-synuclein phosphorylation via reduced protein phosphatase 2A activity. Int J Biochem Cell Biol. 2016;75:34–44.
47. Jeon SM. Regulation and function of AMPK in physiology and diseases. Exp Mol Med. 2016;48:e245.
48. Wu SB, Wu YT, Wu TP, Wei YH. Role of AMPK-mediated adaptive responses in human cells with mitochondrial dysfunction to oxidative stress. Biochim Biophys Acta. 2014;1840:1331–44.
49. Zhang M, Deng YN, Zhang JY, Liu J, Li YB, Su H, et al. SIRT3 protects rotenone-induced injury in SH-SY5Y cells by promoting autophagy through the LKB1-AMPK-mTOR pathway. Aging Dis. 2018;9:273–86.
50. Ramalingam M, Huh YJ, Lee YI. The impairments of alpha-synuclein and mechanistic target of rapamycin in rotenone-induced SH-SY5Y cells and mice model of Parkinson's disease. Front Neurosci. 2019;13:1028.

51. Marin TL, Gongol B, Zhang F, Martin M, Johnson DA, Xiao H, et al. AMPK promotes mitochondrial biogenesis and function by phosphorylating the epigenetic factors DNMT1, RBBP7, and HAT1. Sci Signal. 2017;10:eaaf7478.
52. Chaube B, Malvi P, Singh SV, Mohammad N, Viollet B, Bhat MK. AMPK maintains energy homeostasis and survival in cancer cells via regulating p38/PGC-1alpha-mediated mitochondrial biogenesis. Cell Death Disco. 2015;1:15063.
53. Irrcher I, Ljubicic V, Kirwan AF, Hood DA. AMP-activated protein kinase-regulated activation of the PGC-1alpha promoter in skeletal muscle cells. PLoS One. 2008;3:e3614.
54. Jager S, Handschin C, St-Pierre J, Spiegelman BM. AMP-activated protein kinase (AMPK) action in skeletal muscle via direct phosphorylation of PGC-1alpha. Proc Natl Acad Sci U S A. 2007;104:12017–22.
55. Vucicevic L, Misirkic M, Janjetovic K, Vilimanovich U, Sudar E, Isenovic E, et al. Compound C induces protective autophagy in cancer cells through AMPK inhibition-independent blockade of Akt/mTOR pathway. Autophagy. 2011;7:40–50.
56. Moon JH, Jeong JK, Hong JM, Seol JW, Park SY. Inhibition of autophagy by captopril attenuates prion peptide-mediated neuronal apoptosis via AMPK activation. Mol Neurobiol. 2019;56:4192–202.
57. Meley D, Bauvy C, Houben-Weerts JH, Dubbelhuis PF, Helmond MT, Codogno P, et al. AMP-activated protein kinase and the regulation of autophagic proteolysis. J Biol Chem. 2006;281:34870–9.
58. Filomeni G, Graziani I, De Zio D, Dini L, Centonze D, Rotilio G, et al. Neuroprotection of kaempferol by autophagy in models of rotenone-mediated acute toxicity: possible implications for Parkinson's disease. Neurobiol Aging. 2012;33:767–85.